



Dancing *Volvox*: Hydrodynamic Bound States of Swimming Algae

Knut Drescher,¹ Kyriacos C. Leptos,¹ Idan Tuval,¹ Takuji Ishikawa,² Timothy J. Pedley,¹ and Raymond E. Goldstein¹

¹*Department of Applied Mathematics and Theoretical Physics, University of Cambridge, Cambridge CB3 0WA, United Kingdom*

²*Department of Bioengineering and Robotics, Tohoku University, Sendai 980-8579, Japan*

(Received 14 January 2009; published 20 April 2009)

The spherical alga *Volvox* swims by means of flagella on thousands of surface somatic cells. This geometry and its large size make it a model organism for studying the fluid dynamics of multicellularity. Remarkably, when two nearby *Volvox* colonies swim close to a solid surface, they attract one another and can form stable bound states in which they “waltz” or “minuet” around each other. A surface-mediated hydrodynamic attraction combined with lubrication forces between spinning, bottom-heavy *Volvox* explains the formation, stability, and dynamics of the bound states. These phenomena are suggested to underlie observed clustering of *Volvox* at surfaces.

DOI: 10.1103/PhysRevLett.102.168101

PACS numbers: 47.63.Gd, 87.17.Jj, 87.18.Ed

Long after he made his great contributions to microscopy and started a revolution in biology, Antony van Leeuwenhoek peered into a drop of pond water and discovered one of nature’s geometrical marvels [1]. This was the freshwater alga which, years later, in the very last entry of his great work on biological taxonomy, Linnaeus named *Volvox* [2] for its characteristic spinning motion about a fixed body axis. *Volvox* is a spherical colonial green alga (Fig. 1), with thousands of biflagellated cells anchored in a transparent extracellular matrix (ECM) and daughter colonies inside the ECM. Since the work of Weismann [3], *Volvox* has been seen as a model organism in the study of the evolution of multicellularity [4–6].

Because it is spherical, *Volvox* is an ideal organism for studies of biological fluid dynamics, being an approximate realization of Lighthill’s “squirmers” model [7] of self-propelled bodies having a specified surface velocity. Such models have elucidated nutrient uptake at high Péclet numbers [6,8] by single organisms, and pairwise hydrodynamic interactions between them [9]. Volvocine algae may also be used to study *collective* dynamics of self-propelled objects [10], complementary to bacterial suspensions (*E. coli*, *B. subtilis*) exhibiting large-scale coherence in thin films [11] and bulk [12].

While investigating *Volvox* suspensions in glass-topped chambers, we observed stable bound states, in which pairs of colonies orbit each other near the chamber walls. *Volvox* is “bottom-heavy” due to clustering of daughter colonies in the posterior, so an isolated colony swims upward with its axis vertical, rotating clockwise (viewed from above) at an angular frequency $\omega \sim 1$ rad/s for a radius $R \sim 150 \mu\text{m}$. When approaching the chamber ceiling, two *Volvox* colonies are drawn together, nearly touching while spinning, and they “waltz” about each other clockwise [Fig. 1(a)] at an angular frequency $\Omega \sim 0.1$ rad/s. When *Volvox* have become too heavy to maintain upswimming, two colonies hover above one another near the chamber bottom, oscillating laterally out of phase in a “minuet”

dance. Both dances can last many tens of minutes or even several hours. Although the orbiting component of the waltzing is reminiscent of vortex pairs in inviscid fluids, the attraction and the minuet are not, and as the Reynolds number is ~ 0.03 , inertia is negligible.

While one might imagine that signalling and chemotaxis could result in these bound states, a combination of experiment, theory, and numerical computations is used here to show that they arise instead from the interplay of short-range lubrication forces between spinning colonies and surface-mediated hydrodynamic interactions [13], known to be important for colloidal particles [14,15] and bacteria [16]. We conjecture that flows driving *Volvox* clustering at surfaces enhance the probability of fertilization during the sexual phase of their life cycle.

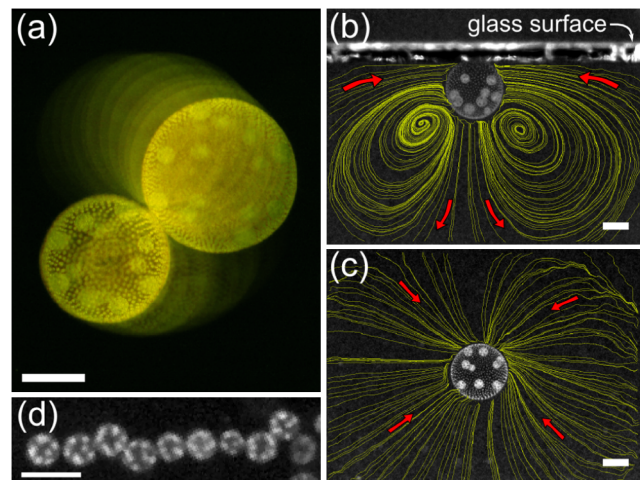


FIG. 1 (color online). Waltzing of *V. carteri*. (a) Top view. Superimposed images taken 4 s apart, graded in intensity. (b) Side, and (c) top views of a colony swimming against a cover slip, with fluid streamlines. Scales are $200 \mu\text{m}$. (d) A linear *Volvox* cluster viewed from above (scale is 1 mm).

Volvox carteri f. *nagariensis* EVE strain (a subclone of HK10) were grown axenically in SVM [6,17] in diurnal growth chambers with sterile air bubbling, in a daily cycle of 16 h in cool white light (~ 4000 lux) at 28°C and 8 h in the dark at 26°C . Swimming was studied in a dual-view system (Fig. 2) [18], consisting of two identical assemblies, each a CCD camera (Pike 145B, Allied Vision Technologies, Germany) and a long-working distance microscope (InfiniVar CMS-2/S, Infinity Photo-Optical, Colorado). Dark-field illumination used 102 mm diameter circular LED arrays (LFR-100-R, CCS Inc., Kyoto) with narrow bandwidth emission at 655 nm, to which *Volvox* is insensitive [19]. Thermal convection induced by the illumination was minimized by placing the $2 \times 2 \times 2$ cm sample chamber, made from microscope slides held together with UV-curing glue (Norland), within a stirred, temperature-controlled water bath. A glass cover slip glued into the chamber provided a clean surface [Fig. 1(b)] to induce bound states. Particle imaging velocimetry (PIV) studies (Dantec Dynamics, Skovlunde, Denmark) showed that the r.m.s convective velocity within the sample chamber was $\lesssim 5 \mu\text{m/s}$.

Four aspects of *Volvox* swimming are important in the formation of bound states, each associated, in the far field, with a distinct singularity of Stokes flow: (i) negative buoyancy (Stokeslet), (ii) self-propulsion (stresslet), (iii) bottom-heaviness (rotlet), and spinning (rotlet doublet). During the 48 h life cycle, the number of somatic cells is constant; only their spacing increases as new ECM is added to increase the colony radius. This slowly changes the speeds of sinking, swimming, self-righting, and spinning, allowing exploration of a range of behaviors. The upswimming velocity U was measured with side views in the dual-view apparatus. The *Volvox* density was determined by arresting self-propulsion through transient deflagellation with a pH shock [6,20], and measuring sedimentation. The settling velocity $V = 2\Delta\rho g R^2/9\eta$,

with g the acceleration of gravity and η the fluid viscosity, yields the density offset $\Delta\rho = \rho_c - \rho$ between the colony and water. Bottom-heaviness implies a distance ℓ between the centers of gravity and geometry, measured by allowing *Volvox* to roll off a guide in the chamber and monitoring the axis inclination angle θ with the vertical. This angle obeys $\zeta_r \dot{\theta} = -(4\pi R^3 \rho_c g \ell/3) \sin\theta$, where $\zeta_r = 8\pi\eta R^3$ is the rotational drag coefficient, leading to a relaxation time $\tau = 6\eta/\rho_c g \ell$ [21]. The rotational frequencies ω_0 of free-swimming colonies were obtained from movies, using daughter colonies as markers.

Figure 3 shows the four measured quantities (U , V , ω_0 , τ) and the deduced density offset $\Delta\rho$. In the simplest model [6], locomotion derives from a uniform force per unit area $\mathbf{f} = (f_\theta, f_\phi)$ exerted by flagella tangential to the colony surface. Balancing the net force $\int dS \mathbf{f} \cdot \hat{\mathbf{z}} = \pi^2 f_\theta R^2$ against the Stokes drag and negative buoyancy yields $f_\theta = 6\eta(U + V)/\pi R$. Balancing the flagellar torque $\int dS R(\hat{\mathbf{r}} \times \mathbf{f}) \cdot \hat{\mathbf{z}} = \pi^2 f_\phi R^3$ against viscous rotational torque $8\pi\eta R^3 \omega_0$ yields $f_\phi = 8\eta\omega_0/\pi$. These components are shown in Fig. 3(f), where we used a linear parameterization of the upswimming data [Fig. 3(a)] to obtain an estimate of U over the entire radius range. The typical force density f_θ corresponds to several pN per flagellar pair [6], while the relative smallness of f_ϕ is a consequence of the $\sim 15^\circ$ tilt of the flagellar beating plane with respect to the colonial axis [22,23].

Using the measured parameters, it is possible to characterize both bound states. Figure 4(c) shows data from measured tracks of 60 pairs of *Volvox*, as they fall together to form the waltzing bound state. The data collapse when the intercolony separation r , normalized by \bar{R} , the mean of

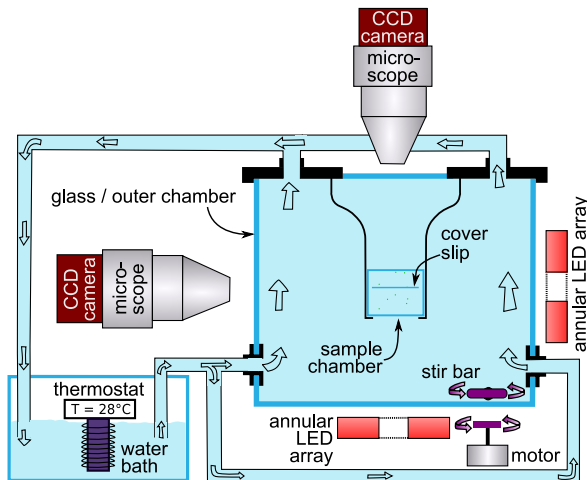


FIG. 2 (color online). Dual-view apparatus.

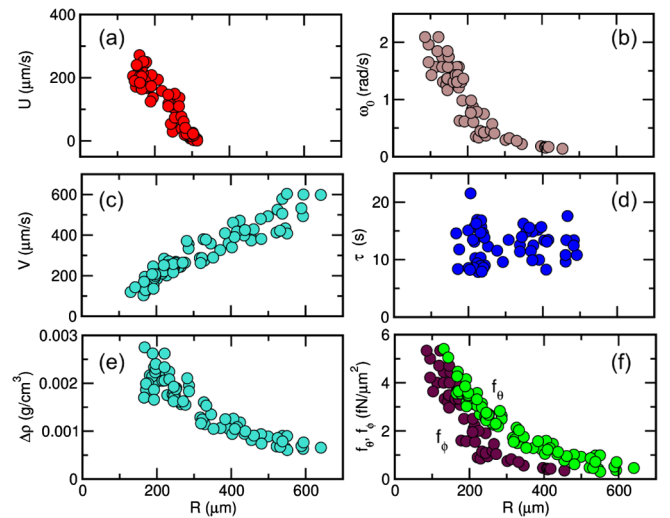


FIG. 3 (color online). Swimming properties of *V. carteri* as a function of radius. (a) upswimming speed, (b) rotational frequency, (c) sedimentation speed, (d) bottom-heaviness reorientation time, (e) density offset, and (f) components of average flagellar force density.

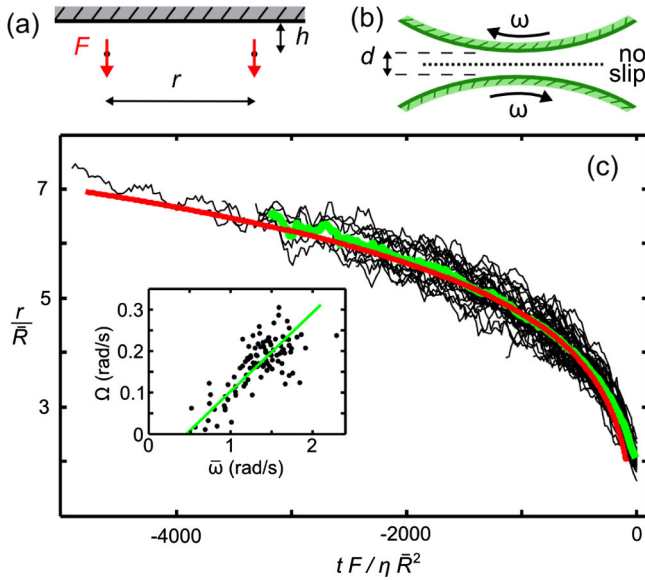


FIG. 4 (color online). Waltzing dynamics. Geometry of (a) two interacting Stokeslets (side view) and (b) nearby spinning colonies (top view). (c) Radial separation r , normalized by mean colony radius, as a function of rescaled time for 60 events (black). Running average (green) compares well with predictions of the singularity model (red). Inset shows orbiting frequency Ω as a function of mean spinning frequency $\bar{\omega}$, and linear fit.

the two participating colonies' radii, is plotted as a function of rescaled time from contact. The waltzing frequency Ω is linear in the mean spinning frequency of the pair $\bar{\omega}$. These two ingredients of the waltzing bound state, “infalling” and orbiting, can be understood, respectively, by far-field features of mutually advected singularities and near-field effects given by lubrication theory, which will now be considered in turn.

Infalling.—When swimming against an upper surface, the net thrust induced by the flagellar beating is not balanced by the viscous drag on the colony, as the colony is at rest, resulting in a net downwards force on the fluid. The fluid response to such a force may be modeled as a Stokeslet normal to and at a distance h from a no-slip surface [13], forcing fluid in along the surface [Fig. 1(c)] and out below the colony, with a toroidal recirculation. Seen in cross section with PIV, the velocity field of a single colony has precisely this appearance [Fig. 1(b)]. This flow produces the attractive interaction between colonies; Squires has proposed a similar scenario in the context of electrophoretic levitation [24].

The motion of a pointlike object at \mathbf{x}_i , with axis orientation \mathbf{p}_i and net velocity \mathbf{v}_i from self-propulsion and buoyancy, due to the fluid velocity \mathbf{u} and vorticity $\nabla \times \mathbf{u}$ generated by the other self-propelled objects, obeys

$$\begin{aligned} \dot{\mathbf{x}}_i &= \mathbf{u}(\mathbf{x}_i) + \mathbf{v}_i, \\ \dot{\mathbf{p}}_i &= \frac{1}{\tau} \mathbf{p}_i \times (\hat{\mathbf{z}} \times \mathbf{p}_i) + \frac{1}{2} (\nabla \times \mathbf{u}) \times \mathbf{p}_i. \end{aligned} \quad (1)$$

Assuming that for the infalling, $\mathbf{v}_i = \dot{\mathbf{p}}_i = 0$, and that $\mathbf{u}(\mathbf{x}_i)$ are due to Stokeslets of strength $F = 6\pi\eta R(U + V)$, Eq. (1) may be reduced, in rescaled coordinates $\tilde{r} = r/h$ and $\tilde{t} = tF/\eta h^2$ with $h = \bar{R}$, to [24]

$$\frac{d\tilde{r}}{d\tilde{t}} = -\frac{3}{\pi} \frac{\tilde{r}}{(\tilde{r}^2 + 4)^{5/2}}. \quad (2)$$

Integration of (2) shows good parameter-free agreement with the experimental trajectories of nearby pairs [Fig. 4(c)]. Large perturbations to a waltzing pair by a third nearby colony can disrupt it by strongly tilting the colony axes, suggesting that bottom-heaviness confers stability. This is confirmed by a linear stability analysis [23].

Orbiting.—As *Volvox* colonies move together under the influence of the wall-induced attractive flows [Fig. 1(b)], orbiting becomes noticeable only when their separation d is $\lesssim 30 \mu\text{m}$; their spinning frequencies also decrease very strongly with decreasing separation. This arises from viscous torques associated with the thin fluid layer between two colonies [Fig. 4(b)]. We assume that in the thin fluid layer, the spinning *Volvox* colonies can be modeled as rigid spheres, ignoring the details of the overlapping flagella layers. For two identical colonies, ignoring the anterior-posterior “downwash,” and considering only the region where the fluid layer is thin, the plane perpendicular to the line connecting their centers is a locus of zero velocity, as with a no-slip wall. Appealing to known asymptotic results [25], we obtain the torque $\mathcal{T} = -(2/5) \ln(d/2R) \zeta_r \omega$ and a lateral force $\mathcal{F} = (1/10) \ln(d/2R) \zeta_r \omega / R$ on the sphere, where $\omega < \omega_0$ is the spinning frequency of a colony in the bound state. The rotational slowing of the self-propelled colony has an effect on the fluid that may be approximated by a rotlet of strength \mathcal{T} at its center. From the flow field of a rotlet perpendicular to a horizontal no-slip wall [13] and the lateral force \mathcal{F} , we then deduce the orbiting frequency

$$\Omega \approx 0.069 \ln\left(\frac{d}{2R}\right) \bar{\omega}. \quad (3)$$

Typical values of d and R give a slope of ≈ 0.14 – 0.19 for the $\Omega - \bar{\omega}$ line, consistent with the experimental fit of 0.19 ± 0.05 [Fig. 4(c)]. The nonzero intercept is likely due to lubrication friction against the ceiling [23].

A second and more complex type of bound state, the “minuet,” is found when the upswimming just balances the settling [at $R \approx 300 \mu\text{m}$, see Fig. 3(a)], and *Volvox* colonies hover at a fixed distance above the chamber bottom. In this mode (Fig. 5) colonies stacked one above the other oscillate back and forth about a vertical axis. The mechanism of oscillation is the instability of the perfectly aligned state due to the vorticity from one colony rotating the other, whose swimming brings it back, with the restoring torques from bottom-heaviness conferring stability. Studies of the coupled dynamics of \mathbf{x}_i and \mathbf{p}_i show that when the orientational relaxation time τ is below a thresh-

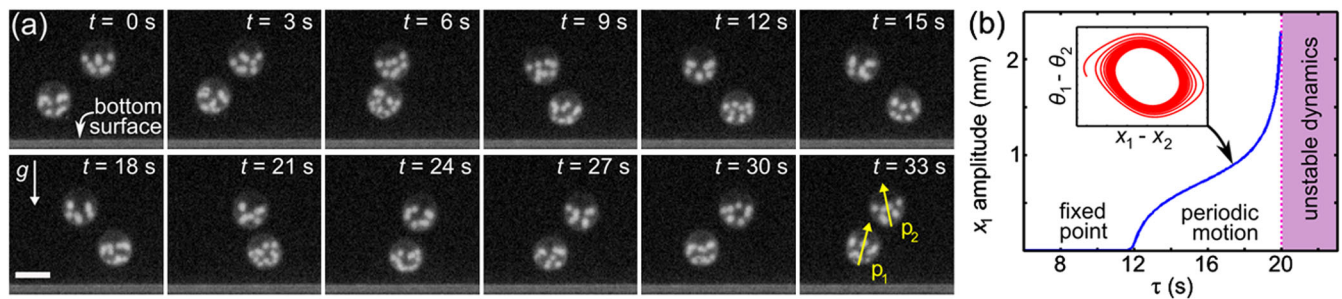


FIG. 5 (color online). “Minuet” bound state. (a) Side views 3 s apart of two colonies near the chamber bottom. Arrows indicate the anterior-posterior axes \mathbf{p}_i at angles θ_i to vertical. Scale bar is $600 \mu\text{m}$. (b) Bifurcation diagram, and phase portrait (inset), showing a limit cycle, with realistic model parameters $F = 6\pi\eta RV$, $R = 300 \mu\text{m}$, $h_1 = 450 \mu\text{m}$, $h_2 = 1050 \mu\text{m}$.

old, the stacked arrangement is stable, while for τ larger, there is a Hopf bifurcation to limit-cycle dynamics [Fig. 5(b)]. In these studies, lubrication effects were ignored, $\dot{\mathbf{x}}_i$ was restricted to be in one horizontal dimension only, and \mathbf{x}_i were at fixed heights h_i above the wall. The flow \mathbf{u} was taken to be due to vertically oriented Stokeslets at \mathbf{x}_i , of magnitude F , equal to the gravitational force on the *Volvox*.

Hydrodynamic bound states, such as those described here, may have biological significance. When environmental conditions deteriorate, *Volvox* colonies enter a sexual phase of spore production to overwinter. Field studies show that bulk *Volvox* concentrations n are $< 1 \text{ cm}^{-3}$ [26], with male/female ratio of $\sim 1/10$, and ~ 100 sperm packets/male. Under these conditions, the mean encounter time for females and sperm packets is a substantial fraction of the life cycle. The kinetic theory mean-free path $\lambda = 1/\sqrt{2}n\pi(R + R_{\text{sp}})^2 \times 10/100$, with $R = 150 \mu\text{m}$ for females, and $R_{\text{sp}} = 15 \mu\text{m}$ for sperm packets, is $\lambda \sim 1 \text{ m}$, implying a mean encounter time $> 2 \text{ h}$ [27]. This suggests that another mechanism for fertilization could be at work, with previous studies having excluded chemoattraction in this system [28]. At naturally occurring concentrations, more than one *Volvox* may partake in the waltzing bound state, leading to large arrays [Fig. 1(d)]. In such clusters, formed at the air-water interface, the recirculating flows would decrease the encounter times to seconds or minutes, clearly increasing the chance of sperm packets finding their target. Studies are underway to examine this possibility.

We thank D. Vella, S. Alben, and C. A. Solari for key observations, A. M. Nedelcu for algae, and support from the BBSRC, DOE, and the Schlumberger Chair Fund.

-
- [1] A. van Leeuwenhoek, Phil. Trans. R. Soc. London **22**, 509 (1700).
 [2] C. Linnaeus, *Systema Naturae* (Impensis Laurentii Salvii, Stockholm, 1758), 10th ed., p. 820.
 [3] A. Weismann, *Essays Upon Heredity and Kindred Biological Problems* (Clarendon Press, Oxford, 1891).

- [4] D. L. Kirk, *Volvox: Molecular-genetic Origins of Multicellularity and Cellular Differentiation* (Cambridge University Press, Cambridge, 1998).
 [5] D. L. Kirk, *BioEssays* **27**, 299 (2005).
 [6] C. A. Solari *et al.*, Proc. Natl. Acad. Sci. U.S.A. **103**, 1353 (2006); M. B. Short *et al.*, Proc. Natl. Acad. Sci. U.S.A. **103**, 8315 (2006); C. A. Solari, J. O. Kessler, and R. E. Michod, Am. Nat. **167**, 537 (2006).
 [7] M. J. Lighthill, Commun. Pure Appl. Math. **5**, 109 (1952).
 [8] V. Magar, T. Goto, and T. J. Pedley, Q. J. Mech. Appl. Math. **56**, 65 (2003).
 [9] T. Ishikawa and M. Hota, J. Exp. Biol. **209**, 4452 (2006); T. Ishikawa, M. P. Simmonds, and T. J. Pedley, J. Fluid Mech. **568**, 119 (2006).
 [10] T. Ishikawa and T. J. Pedley, Phys. Rev. Lett. **100**, 088103 (2008); T. Ishikawa, J. T. Locei, and T. J. Pedley, J. Fluid Mech. **615**, 401 (2008).
 [11] X.-L. Wu and A. Libchaber, Phys. Rev. Lett. **84**, 3017 (2000); A. Sokolov, *et al.*, Phys. Rev. Lett. **98**, 158102 (2007).
 [12] C. Dombrowski, *et al.*, Phys. Rev. Lett. **93**, 098103 (2004).
 [13] J. R. Blake, Proc. Cambridge Philos. Soc. **70**, 303 (1971); J. R. Blake and A. T. Chwang, J. Eng. Math. **8**, 23 (1974).
 [14] H. J. Keh and J. L. Anderson, J. Fluid Mech. **153**, 417 (1985).
 [15] E. R. Dufresne *et al.*, Phys. Rev. Lett. **85**, 3317 (2000).
 [16] A. P. Berke *et al.*, Phys. Rev. Lett. **101**, 038102 (2008).
 [17] D. L. Kirk and M. M. Kirk, Dev. Biol. **96**, 493 (1983).
 [18] K. Drescher, K. Leptos, and R. E. Goldstein, Rev. Sci. Instrum. **80**, 014301 (2009).
 [19] H. Sakaguchi and K. Iwasa, Plant Cell Physiol. **20**, 909 (1979).
 [20] G. B. Witman *et al.*, J. Cell Biol. **54**, 507 (1972).
 [21] T. J. Pedley and J. O. Kessler, Annu. Rev. Fluid Mech. **24**, 313 (1992).
 [22] H. J. Hoops, Protoplasma **199**, 99 (1997).
 [23] K. Drescher *et al.* (to be published).
 [24] T. Squires, J. Fluid Mech. **443**, 403 (2001).
 [25] S. Kim and S. J. Karrila, *Microhydrodynamics: Principles and Selected Applications* (Dover, New York, 2005).
 [26] F. DeNoyelles, Jr., Ph.D. thesis, Cornell Univ., 1971.
 [27] T. Ishikawa and T. J. Pedley, J. Fluid Mech. **588**, 437 (2007).
 [28] S. J. Coggging *et al.*, Journal of Phycology **15**, 247 (1979).